

II. s-LLGS AND FPE ANALYSES

s-LLGS and FPE-based analyses has been widely used to characterize MTJ switching. This section introduces the equations and presents the proposed FPE solvers. Figure 1 describes the proposed toolbox, consisting of an s-LLGS compact model [7], a FVM FPE solver, an analytical FPE solver based on [11] and optimization tools using global minimization [12]. The s-LLGS compact model computes stochastic random transient walks based on a set of MTJ parameters. FPE solvers evolve a known initial magnetization probability distribution $\rho_0(\theta)$, computing the magnetization probability at a given time $\rho(\tau, \theta)$. Finally, the optimization module solves for MTJ statistics and fits parameters to achieve a target error rate.

A. MTJ Stochasticity: Origin in s-LLGS

The temporal evolution of MTJ magnetization \mathbf{m} can be described as a monodomain nanomagnet influenced by external and anisotropy fields, thermal noise and STT [5], [6], ruled by the s-LLGS equations [5] in I.S.U.

$$\frac{d\mathbf{m}}{dt} = -\gamma' \mathbf{m} \times \mathbf{H}_{eff} + \alpha \gamma' \mathbf{m} \times \frac{d\mathbf{m}}{dt} + \gamma' \beta \epsilon (\mathbf{m} \times \mathbf{m}_p \times \mathbf{m}) - \gamma' \beta \epsilon' (\mathbf{m} \times \mathbf{m}_p) \quad (1)$$

where α and γ are the Gilbert damping factor and gyromagnetic ratio respectively, related by $\gamma' = \frac{\gamma \mu_0}{1 + \alpha^2}$, P is the polarization factor, M_s is the magnetization saturation, I is the current flowing through the MTJ volume V , m_p is the pinned-layer unitary polarization direction and β, ϵ and ϵ' refer to the STT field parameters [5]. The effective magnetic field for a Perpendicular Magnetic Anisotropy (PMA) is defined by the anisotropy field, the external field and the thermal induced field $\mathbf{H}_{eff} = \mathbf{H}_{ani} + \mathbf{H}_{ext} + \mathbf{H}_{th}$. The thermal fluctuations induced field is expressed as

$$\mathbf{H}_{th} = \mathcal{N}(\mathbf{0}, \mathbf{1}) \sqrt{\frac{2K_B T \alpha}{\gamma' M_s V \Delta t}} \quad (2)$$

where K_B is the Boltzmann constant and $\mathcal{N}(\mathbf{0}, \mathbf{1})$ is a Gaussian random vector with components in x, y, z meeting conditions from [6], [13].

B. Fokker-Planck Equation

Fokker-Planck (advection-diffusion) Equation has been widely used as a tool to establish the probability density function (PDF) of the MTJ magnetization at a given time [2], [8]–[10], being the SDE formalized as

$$\begin{aligned} \frac{\partial \rho}{\partial \tau} &= -\frac{1}{\sin(\theta)} \frac{\partial}{\partial \theta} \left[\sin^2(\theta) (i - h - \cos(\theta)) \rho - \frac{\sin(\theta)}{2\Delta} \frac{\partial \rho}{\partial \theta} \right] \\ &= \frac{\partial}{\partial \theta} \left[U(\theta) \rho + D(\theta) \frac{\partial \rho}{\partial \theta} \right] \end{aligned} \quad (3)$$

where $i = \frac{I}{I_c}$, $h = \frac{\mathbf{H}_{ext} \cdot \mathbf{z}}{H_k^{eff}}$ are constant vectors with zero x, y components, $\tau = \frac{t}{\tau_d}$, $I_c = \frac{\alpha H_k^{eff}}{\epsilon \beta}$, $\tau_d = \frac{1}{\alpha \gamma' H_k^{eff}}$ and H_k^{eff} is the effective z -component of the shape, interfacial, bulk and voltage-controlled anisotropy. As seen in Equation (3), FPE

definition does not involve any stochastic fields. The advection $U(\theta)$ term is responsible for the drift of the distribution while the finite-temperature effects are determined by its initial state $\rho(\theta)|_{\tau=0} = \rho_0(\theta)$, and within its diffusion term $D(\theta)$ [14].

III. IMPLEMENTED FPE SOLVERS

Prior work numerically solves the FPE through finite differences or finite element methods [2], [8], [9] or analytical solutions [11]. This work implements two different FPE solvers. The first is a numerical FVM approach, which guarantees the conservative properties over the computed magnetization flux [10], [15]. This method solves on non-uniform meshes using an adaptive *upwinding* exponential fitting scheme for the diffusion coefficient, and combines explicit and implicit methods through Crank-Nicolson, preserving stability while increasing accuracy [15].

The FVM solver's computational load limits its practical applicability to thermal regime scenarios where $I \ll I_c$. To circumvent this limitation, this work implements a second solver following [11], where an analytical solution to Equation (3) is presented after expanding ρ as a Legendre polynomial series

$$\frac{\partial \rho}{\tau} = \sum_{n=0}^{\infty} \sum_{k=-2}^2 r_n a_{n+k, n} P_{n+k}. \quad (4)$$

Limiting the series to its first N coefficients $a_{i,j} \in [0, N]$, we can form the pentadiagonal matrix A [11] leading to:

$$\frac{\partial \mathbf{r}(\tau)}{\partial \tau} = \mathbf{A} \mathbf{r}(\tau) \implies \mathbf{r}(\tau) = e^{\mathbf{A}\tau} \mathbf{r}(\mathbf{0}), \quad (5)$$

where $\mathbf{r}(\tau)$ are the Legendre expansion coefficients of $\rho(\tau)$, and $\mathbf{r}(\mathbf{0})$ are the Legendre expansion coefficients of ρ_0 , the magnetization initial state. The system described by Equations (4, 5) is implemented using `SciPy` [12], allowing the computation of long FPE evolutions with simple matrix exponentiation and multiplication operations.

Figure 2 shows the evolution of $\rho(\theta)$, switching from 0 to π in response to applied current. With sufficient resolution, both solvers produce closely matched results. Runtime comparison shows that both FPE solvers, even at high resolution, are well below the runtime of a single s-LLGS transient evaluation – accurate statistical simulation for low error rates would need billions of such evaluations. The implemented solvers therefore offer a practical tool for evaluating MTJ statistics over a wide accuracy/runtime span. The analytical FPE accuracy gets determined by the number N of coefficients, being N 200 sufficient, and then computationally-scaling $O(1)$ with the simulated time independently of the θ dimension. On the contrary, the accuracy of FVM FPE relies on the grid t_s time and $\frac{\pi}{M}$ theta precision – which involves $O(n^2)$ runtime.

IV. CASE STUDY

WER/RER dependence on MTJ parameters has been actively investigated, and works like [9], [11] emphasize the importance of FPE as its underlying tool. Circuit designers

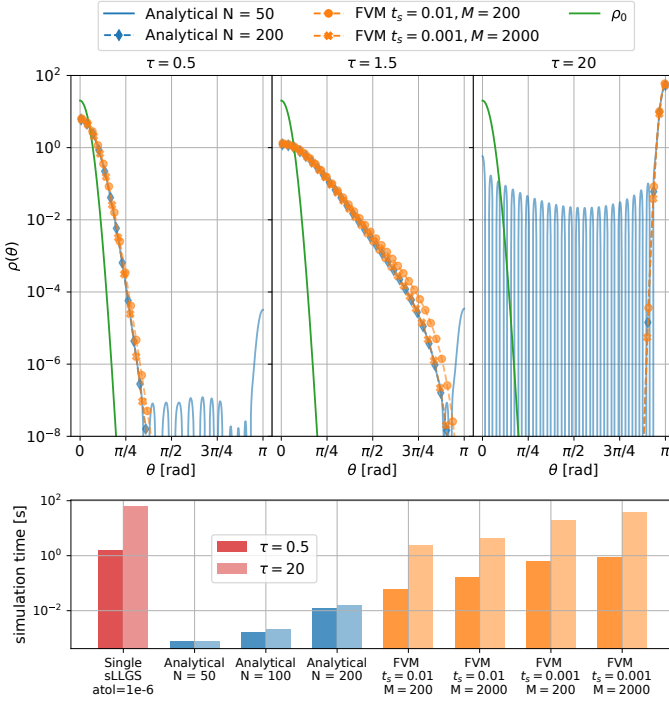


Fig. 2. FPE solvers analysis for an MTJ with $H_k^{eff} = 177415 \frac{A}{m}$, $\Delta = 63$, $\alpha = 0.01$, $M_s = 1.2e6 \frac{A}{m}$. The top graph shows the effect of resolution on the temporal evolution of Eq. (3). In the bottom graph the FPE computation times are compared against a single s-LLGS transient.

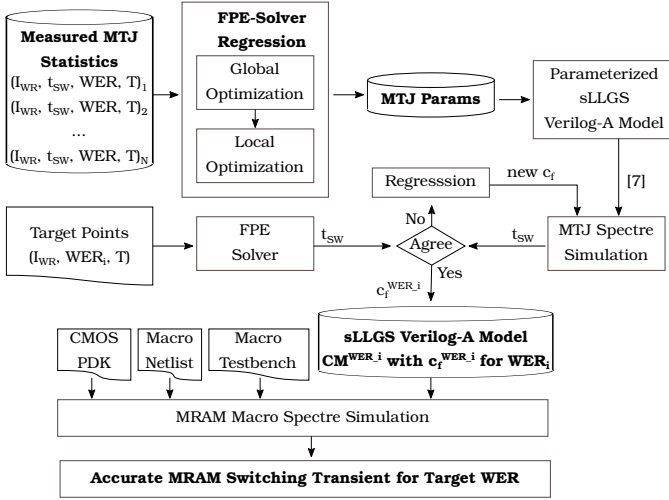


Fig. 3. Proposed methodology for MTJ stochastic behavior analysis and accurate s-LLGS Verilog-A model parameterization for WER switching transient simulation.

require calibrated MRAM compact models reflecting the behavior of MTJ technologies at different statistical operating points: mean behavior or $WER_{0.5}$, WER_{1e-6} or WER_{1e-8} stochastic corner behaviour. Finding the optimum set of physical parameters that best fit a collection of WER points as a function of a current pulse width and amplitude can be seen as a complex NP-hard problem where a black-box module computes the required time-to-switch under a given current.

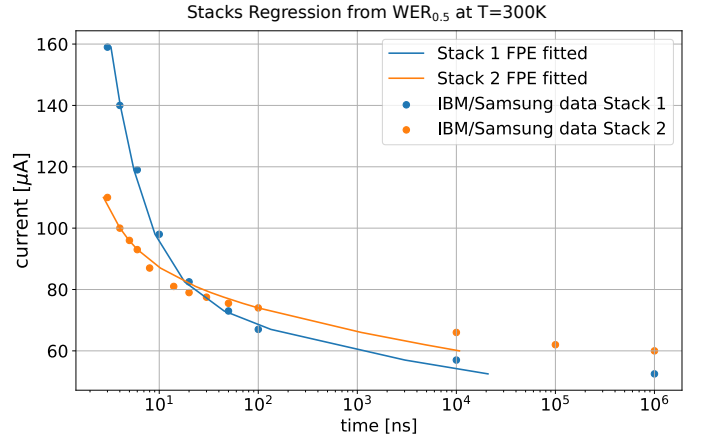


Fig. 4. Stacks 1 and 2 for fast switching MTJs presented in [14], regressed using the proposed framework.

Figure 3 describes the methodology addressing these problems. For the simpler characterization problem, the FPE solver computes the statistical behavior of a given MTJ operating under known current, pulse width and temperature conditions. On the other hand, the full regression problem requires finding the MTJ parameters that fit known *measured* MTJ statistics – current/time/temperature switching behaviors for measured WER points. Global optimization algorithms followed by local iterations explore the design space minimizing a target curve.

Closing the loop between FPE and the regression problem, our framework implements an optimization module based on heuristic algorithms using SciPy optimize toolbox [12] which outputs the best suited MTJ physical parameters. By applying [7] the corresponding circuit compact models $\{CM_{WER}^i\}$ describing the cell switching transient for WER_i operation points are generated, enabling the circuit designers to simulate such key events. The parameterized models in $\{CM_{WER}^i\}$ share the same physical parameters, and only differ in the fitting parameters $c_f^{WER,i}$ thermal fitting coefficients, referring to the fake thermal stress. The expansion of Equation 1 in spherical coordinates describes m_θ evolution as proportional to $H_{eff}\phi + \alpha H_{eff}\theta$, leaving $\frac{d}{dt} m_\theta \simeq \frac{\gamma'}{1+\alpha^2} H_{eff}\phi$. The model in [7] introduces a fictitious H_{fth} term into $H_{eff}\phi$ to emulate the required statistical H_{th} contribution. The emulated H_{fth} is defined as

$$H_{fth} = c_f \sqrt{\frac{2K_B T \alpha}{\gamma' M_s V \Delta_t}} \phi. \quad (6)$$

A straightforward calibration involving a negligible amount of s-LLGS simulations leads to the set of $c_f^{WER,i}$ coefficients.

A case study using foundry data published in [14] is presented as an applied example. It is worth noticing that though the included *basin hopping* or *simulated annealing* algorithms attempt to find the global minimum efficiently, as in any heuristic achieving good solutions requires sophisticated problem-tailored cooling/sampling schedules. Figure 4 describes the regression results after using the optimizer module – basin hopping global optimization followed by *L-BFGS-B*

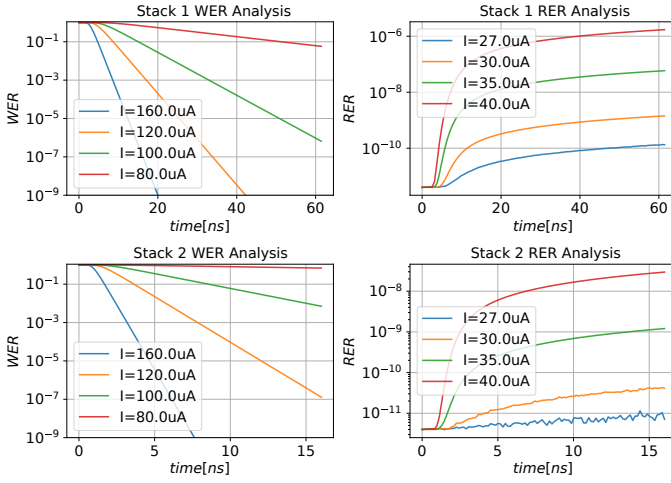


Fig. 5. WER/RER analyses for regressed MTJ stacks [14].

algorithm – fitting to the available $WER_{0.5}$ data points. In this example, the optimization algorithm emphasized the high-current regime as the analyzed stacks were engineered and tested for fast switching [14].

Once the MTJ parameters are regressed, their statistical behaviour can be studied under any conditions using the FPE solvers as shown in Figure 5. WER and RER rates are calculated for different writing and reading currents. It can be noted how Stack 2 is characterized by an easier write-ability, requiring less time to switch in the same current. At low-current regimes Stack 2 tolerates larger currents before flipping the cell during read operations. Such analysis quantifies the impact of MTJ stochasticity taking into account its complex parametric, temperature and current dependencies, helping circuit designers to make informed choices about read/write currents, pulse widths and ECC requirements.

Finally, making use of the regressed parameters and time/current dependence for $WER_{0.5}$, $WER_{10^{-6}}$ and $WER_{10^{-8}}$, the c_f^{WER-i} thermal fitting coefficients are calibrated using single MTJ s-LLGS transient simulation to generate circuit-ready transient models. Figure 6 depicts the simulated transients of Stack 1 and Stack 2 cells accurately describing the switching events.

V. CONCLUSIONS

This work presented a framework for the characterization and analysis of MTJ stochasticity. We implemented and analyzed two FPE solvers (numerical FVM and analytical), and presented an optimization module that orchestrates the efficient computation of MTJ statistics and parameter regression. Finally, we applied the proposal in a case study with published foundry data, demonstrating efficient MTJ parameter regression and the generation of s-LLGS Verilog-A models enabling the simulation of target WER switching transients. The framework code is available upon request.

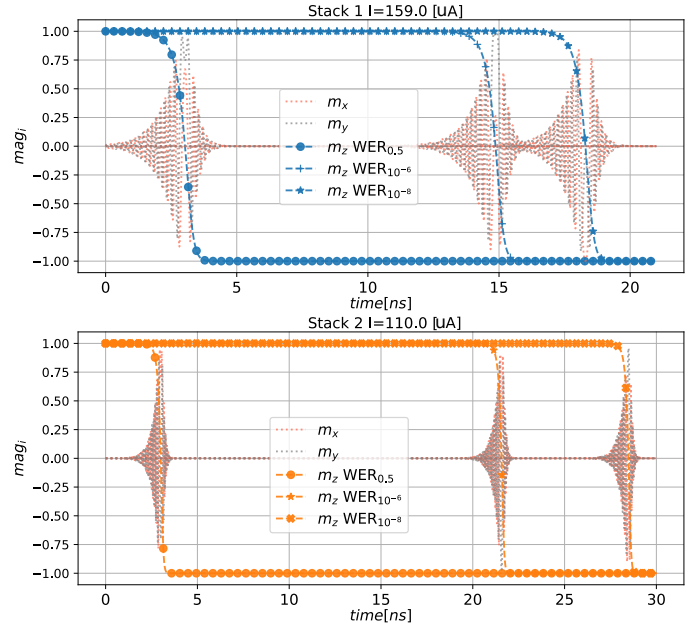


Fig. 6. Transient evaluation for both Stack 1 and 2 [14] at $WER_{0.5}$, $WER_{10^{-6}}$ and $WER_{10^{-8}}$ using [7] compact model. The figure describes the magnetization vector $\mathbf{m}(t)$ decomposed on its three x , y and z components.

VI. ACKNOWLEDGMENTS

The authors would like to thank Milos Milosavljevic and Cyrille Dray for their helpful discussions.

REFERENCES

- [1] H. Lee *et al.*, “Analysis and Compact Modeling of Magnetic Tunnel Junctions Utilizing Voltage-Controlled Magnetic Anisotropy,” *IEEE Trans. Magn.*, vol. 54, no. 4, 2018.
- [2] M. M. Torunbalci *et al.*, “Modular Compact Modeling of MTJ Devices,” *IEEE Trans. Electron Devices*, vol. 65, no. 10, pp. 4628–4634, 2018.
- [3] K. Zhang *et al.*, “Compact Modeling and Analysis of Voltage-Gated Spin-Orbit Torque Magnetic Tunnel Junction,” *IEEE Access*, 2020.
- [4] E. M. Boujamaa *et al.*, “A 14.7Mb/mm² 28nm FDSOI STT-MRAM with Current Starved Read Path, 52Ω/Sigma Offset Voltage Sense Amplifier and Fully Trimmable CTAT Reference,” *IEEE Symp. VLSI Circuits, Dig. Tech. Pap.*, 2020.
- [5] M. J. Donahue *et al.*, “OOMMF user’s guide, version 1.0,” NIST, Gaithersburg, MD, Tech. Rep., 1999.
- [6] S. Ament *et al.*, “Solving the stochastic Landau-Lifshitz-Gilbert-Slonczewski equation for monodomain nanomagnets : A survey and analysis of numerical techniques,” pp. 1–19, 2016.
- [7] F. García-Redondo *et al.*, “A Compact Model for Scalable MTJ Simulation,” in *IEEE Int. Conf. Synth. Model. Anal. Simul. Methods Appl. to Circuit Des., SMACD*, 2021.
- [8] W. H. Butler *et al.*, “Switching distributions for perpendicular spin-torque devices within the macrospin approximation,” *IEEE Trans. Magn.*, vol. 48, no. 12, pp. 4684–4700, 2012.
- [9] Y. Xie *et al.*, “Fokker-Planck Study of Parameter Dependence on Write Error Slope in Spin-Torque Switching,” *IEEE Trans. Elect. Dev.*, 2017.
- [10] Daniel, “danieljfarrell/FVM: Release 0.1.2,” mar 2021.
- [11] M. Tzoufras, “Switching probability of all-perpendicular spin valve nanopillars,” *AIP Adv.*, vol. 8, no. 5, 2018.
- [12] P. Virtanen *et al.*, “SciPy 1.0: fundamental algorithms for scientific computing in Python,” *Nat. Methods*, vol. 17, no. 3, mar 2020.
- [13] W. F. Brown, “Thermal Fluctuations of a Single-Domain Particle,” *Phys. Rev.*, vol. 130, no. 5, pp. 1677–1686, jun 1963.
- [14] G. Hu *et al.*, “Spin-transfer torque MRAM with reliable 2 ns writing for last level cache applications,” *Tech. Dig. - Int. Electron Devices Meet. IEDM*, vol. 2019-Decem, pp. 2019–2022, 2019.
- [15] J. Hundsdoerfer, W. and Verwer, *Numerical Solution of Time-Dependent Advection-Diffusion-Reaction Equations*. Springer B.H., 2007.